A Simple Analytical Model of Low-Frequency Wind-Driven Upwelling on a Continental Slope*

ERIC WOLANSKI

Australian Institute of Marine Science, P.M.B. No. 3, Townsville, M.C., 4810 Australia

(Manuscript received 17 December 1985, in final form 28 March 1986)

ABSTRACT

A simple closed-form analytical solution of a classical coastal upwelling is found in terms of two-dimensional baroclinic waves trapped in a two-layer ocean on a steep continental slope and forced by the wind-driven reversals of currents on an adjoining wide and vertically well-mixed continental shelf. Bottom friction on the continental shelf plays a dominant role. This solution agrees qualitatively with the sparse available records of low-frequency oscillations of currents and temperature on the upper continental slope of the Great Barrier Reef.

1. Introduction

Some continental shelves, like the one of the central region of the Great Barrier Reef of Australia (Fig. 1), are characterized by a wide (width $\approx$ 100 km) shallow (depth $\approx$ 40 m) vertically well-mixed shelf. The shelf slope is very steep. There exists a well-mixed layer, of order 100 m, so that the thermocline is found offshore from the shelf break, virtually at the shelf break.

On the Great Barrier Reef in winter, the system is forced by trade winds from the southeast (i.e., roughly longshore), typically 10 days in duration, and separated by calm periods usually no more than a few days in duration. The horizontal scales of the wind system are much larger than shelf scales. The idealized topography is sketched in Fig. 2d.

In such situations, one expects the longshore wind stress fluctuations to generate upwelling or downwelling of the thermocline over the continental slope. A number of models of such situations have been proposed by Gill and Clarke (1974), Kajiura (1974), Allen (1980), Mysak (1980), Csanady (1982), Clarke and Brink (1985), and others. No simple closed-form solution is available, nor is it always clear if bottom friction plays an important role.

In what follows, a simple analytical closed-form solution is obtained for the response of the system to a transient wind forcing. It is suggested that, when bottom friction is important on the shelf, the vertical oscillations of the thermocline on the upper slope may be driven not by the local wind, but by the reversing currents on the adjoining shelf where friction plays a dominant role.

This solution qualitatively explains one-year long observations from two current meters moored on the continental slope of the Great Barrier Reef.

2. The models

The first model developed assumes a constant depth two-layer ocean and no shelf, and is used only to predict a 90° lag between the wind stress and the currents. The observations suggest a much smaller lag. As a result, another model is developed, assuming a two-layer ocean with a wide shallow well-mixed shelf. This model gives more realistic results.

a. Vertical slope model

First, it will be shown that it is not the local wind on the slope that matters but the fluctuating wind on the adjoining continental shelf. To do this, a two-layer ocean without a shelf is assumed, and the ocean response to a fluctuating wind stress is obtained in terms of trapped waves. The results are a composite of the models and assumptions of Csanady (1982) and Lewis and Reid (1985).

To solve the two-layer situation, it is appropriate to start with the one-layer ocean sketched in Fig. 2a where the definitions of the variables follow those of Csanady. All longshore gradients are neglected in the ocean. The shelf and offshore winds can be assumed to be similar in the trade wind season (Wolanski, 1982). As in Lewis and Reid, the wind stress is decomposed in its various components using a Fourier transform, so that the forcing is provided by a fluctuating longshore wind stress, $\tau = \rho u_*^2 e^{i\omega t}$, where ω is the frequency, u_* the shear velocity, ρ the density, and t the time. In view of the large depths of the ocean, bottom friction can be neglected. This assumption is contrary to the shallow

* Contribution Number 333 from the Australian Institute of Marine Science.

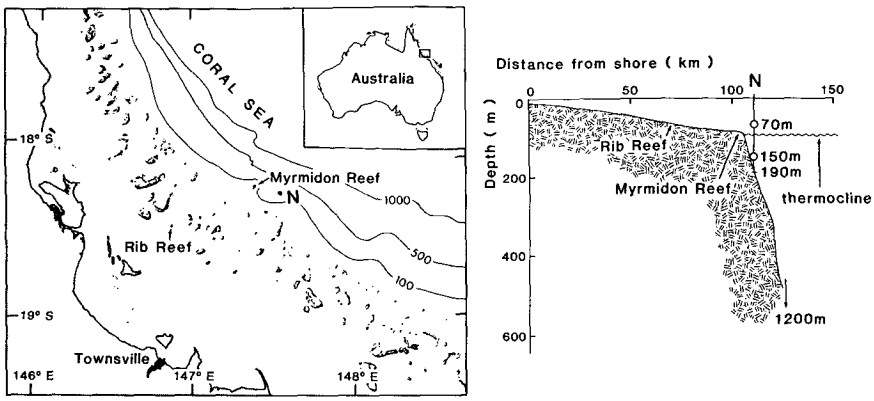

FIG. 1. General location map with depth in m, and sea floor profile with location of current meters.

water model of Lewis and Reid but is in agreement with that of Csanady. The linearized equations of motion are

$$\frac{\partial U}{\partial t} - fV = -c^2 \frac{\partial \zeta}{\partial x} \tag{1}$$

$$\frac{\partial V}{\partial t} + fU = u_*^2 e^{i\omega t} \tag{2}$$

$$\frac{\partial U}{\partial x} + \frac{\partial \zeta}{\partial t} = 0 \tag{3}$$

where U and V are the fluxes, i.e. the depth-integrated cross-shelf and longshore currents, $c^2 = gH$ where g is the acceleration due to gravity and H the total depth, f the Coriolis parameter and ζ the surface displacement. The boundary condition is

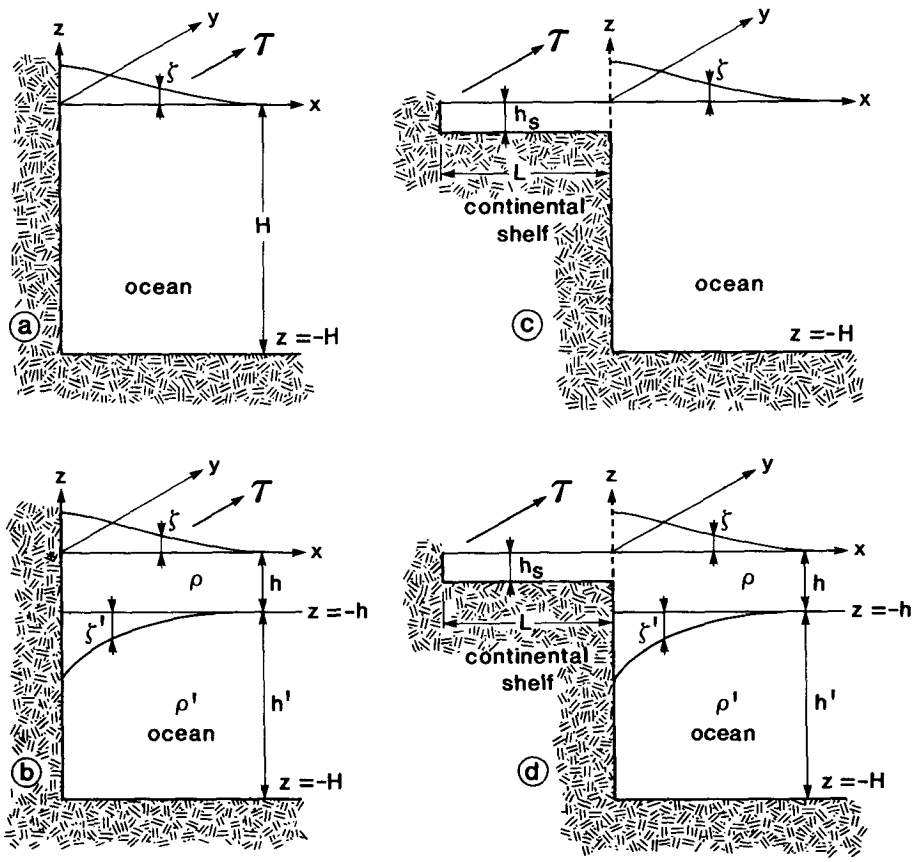

FIG. 2. Various model geometries.

$$U=0 \quad \text{at} \quad x=0. \tag{4}$$

The solution is, if $\zeta \to 0$ at $x \to \infty$,

$$\zeta=-iu_*^2 f e^{lx}e^{i\omega t}/\omega l c^2 \tag{5}$$

$$U=u_*^2 f(1-e^{lx})e^{i\omega t}/(f^2-\omega^2) \tag{6}$$

$$V=iu_*^2 f e^{i\omega t}(\omega^2-f^2e^{lx})/\omega(f^2-\omega^2) \tag{7}$$

where

$$l=-[(f^2-\omega^2)/c^2]^{1/2}<0. \tag{8}$$

Equations (5) to (8) enable one to find readily a solution for the two-layer ocean sketched in Fig. 2b, without a shelf and with an identical wind forcing as above. The currents, integrated over local depth (h for the top layer, h' for the bottom layer) are U and V, and U' and V', respectively, for the top and bottom layers.

There are now barotropic and baroclinic responses. The barotropic response, given the subscript 1, is, from Eqs. (5) to (7),

$$\zeta_1+\zeta_1'=-iu_*^2 f e^{lx}e^{i\omega t}/\omega l c^2 \tag{9}$$

$$V_1+V_1'=iu_*^2 e^{i\omega t}(\omega^2-f^2e^{lx})/\omega(f^2-\omega^2) \tag{10}$$

$$U_1+U_1'=u_*^2 f(1-e^{lx})e^{i\omega t}/(f^2-\omega^2) \tag{11}$$

where

$$U_1'=h'U_1/h, \quad V_1'=h'V_1/h, \quad \zeta_1'=h'\zeta_1/(h+h'); \tag{12}$$

ζ is the free surface displacement and ζ' the thermocline displacement.

The baroclinic response, given the subscript 2, is, from Eqs. (5) to (7),

$$\zeta_2'=-\epsilon\left(\frac{h+h'}{h'}\right)\zeta_2=iu_*^2 e^{i\omega t}\frac{h'}{(h+h')}\frac{fe^{l_2x}}{\omega c_2{}^2 l_2} \tag{13}$$

$$U_2'=-U_2=-u_*^2\frac{h'f}{(h+h')}\frac{(1-e^{l_2x})e^{i\omega t}}{(f^2-\omega^2)} \tag{14}$$

$$V_2'=-V_2=-iu_*^2\frac{h'}{(h+h')}\frac{(\omega^2-f^2e^{l_2x})}{\omega(f^2-\omega^2)}e^{i\omega t} \tag{15}$$

where

$$c_2{}^2=g\epsilon h'h/(h+h'), \quad \epsilon=(\rho'-\rho)/\rho \ll 1,$$

and

$$l_2=-[(f^2-\omega^2)/c_2{}^2]^{1/2}; \tag{16}$$

ρ and ρ' are the densities in the top and bottom layer.

The combined response is

$$\zeta=\zeta_1+\zeta_2, \quad U=U_1+U_2, \quad U'=U_1'+U_2',$$
$$V=V_1+V_2, \quad V'=V_1'+V_2'$$

and is readily obtained from Eqs. (9) to (16).

This model is similar to Csanady (1982) and Lewis and Reid (1985) upwelling models, friction in this case being safely neglected. It is very simple indeed but it shows a number of features that contradict the observations of classical upwelling. For instance, the model predicts that τ and V are 90° out-of-phase while the observations show they are more nearly in phase.

This finding suggests that in some way friction is important. Since the depth on the slope is very large, friction on the slope can still be neglected, but friction on the shallow shelf is a controlling parameter provided a coupling exists between shelf and slope dynamics.

b. *Shelf–ocean coupling*

The proposed two-layer model with a flat shelf is shown in Fig. 2d. Again, to obtain the solution, the response of the one-layer model (Fig. 2c) is needed. Because of the respective length scales (shelf width $\approx$ 100 km $\gg$ internal Rossby radius $\approx$ slope width $\approx$ 10 km), the wind stress is only applied on the shelf.

On the shelf, given the subscript s, friction is dominant (at least on the Great Barrier Reef shelf) since the shelf is shallow. The equations are, following the observations of Wolanski and Bennett (1983),

$$\frac{\partial V_s}{\partial t}\approx u_*^2 e^{i\omega t}-rV_s-g\frac{\partial \zeta_s}{\partial y}-fU_s \tag{17}$$

$$-fV_s=-c_s{}^2\frac{\partial \zeta_s}{\partial x} \tag{18}$$

$$\frac{\partial U_s}{\partial x}+\frac{\partial V_s}{\partial y}=0 \tag{19}$$

subject to $U_s = 0$ at $x = -L$, where r is the friction parameter, $c_s{}^2 = gh_s$, where h_s is the shelf depth and L is the shelf width. The longshore pressure gradient, $-g\partial\eta_s/\partial y$, is not negligible on the shelf. In fact, it forms an essential part of the hydrodynamics of wind-driven shelf currents. This has been shown for a large number of shallow shelves (see a review in Schwing et al., 1985). This has also been found to be true for the Great Barrier Reef (Wolanski and Bennett, 1983; Wolanski and Thomson, 1984; Middleton and Thomson, 1985).

The solution of Eqs. (17) to (19) depends on the boundary conditions. In the Great Barrier Reef, the field data suggests the presence in winter of wind-driven shelf waves, forced from a topographic origin located 400 km further south. It results that at the shelf break ($x = 0$), to zero order in h/H (Wolanski and Bennett, 1983):

$$\zeta_s\approx 0 \tag{20}$$

$$U_s\approx i\alpha e^{i\omega t} \tag{21}$$

where

$$\alpha\approx\frac{Lu_*^2\omega}{c_s(r+i\omega)}e^{(-i\omega y/c_s)}e^{(-ry/c_s)}. \tag{22}$$

Note that ζ_s vanishes only at the shelf break, not on the rest of the shelf, as a result of the coupling between shelf and ocean waters, and then only because of the assumption of a vertical continental slope. The observations (Wolanski and Bennett, 1983) confirm quantitatively this finding, with peak to trough sea level

variations in the "weather band" of order 30 cm at the coast, but typically 1/10 as much at the 100 m isobath. There, the sea level fluctuations are comparable in magnitude to those observed in the Coral Sea at Flinders Reef, located 100 km farther offshore in the Coral Sea. With the available dataset, the influence on the sea level at the shelf break of the wind-driven currents, cannot be separated from that of the ocean forcing.

Note also that α is y-dependent. However, in the case of the central Great Barrier Reef, one is located at a distance y = 400–600 km from the likely topographic origin. With $r \approx 10^{-5}$–10^{-4} s^{-1}, $c_s \approx 230$ km day^{-1} and $\omega \approx 10^{-6}$ s^{-1}, it turns out that the change in the value of α as y varies from 400 to, say, 600 km is quite small, of order 10% of its mean value at 500 km. Thus, as a first approximation, α can be taken to be independent of y. From Eq. (22), α is a complex number. For $r > \omega$, α is practically a real number. For $r = \omega$, α is a complex number of equal real and imaginary parts. Because of the complex reef-studded topography which is believed to increase the value of r (Church et al., 1985; Wolanski et al., 1984), there is some uncertainty on the value of r which is believed to range between 10^{-4} and 10^{-5} s^{-1}. The period of the forcing corresponding to $r \approx \omega$ varies correspondingly between 7.3 and 0.73 days.

Equations (20) to (22) provide the forcing for the dynamical response of the ocean close to the shelf break. Because the forcing is roughly independent of y, it is assumed, in the absence of data, that the response of the ocean close to the shelf break is also independent of y. This assumption may be justified, at least for the case of the Great Barrier Reef, in view of the observations, which were not explained, of Andrews and Furnas (1986) that on the outer shelf the low-frequency bottom-tagging cold water intrusive tongues, when they occur, can be coherent over at least 200 km in the longshore direction.

To solve for the two-layer ocean, the one-layer ocean is needed. The trapped wave solution for the one-layer ocean (Fig. 2c) satisfies the equation

$$\frac{\partial U}{\partial t} - fV = -c^2 \frac{\partial \zeta}{\partial x} \tag{23}$$

$$\frac{\partial V}{\partial t} + fU = 0 \tag{24}$$

$$\frac{\partial U}{\partial x} + \frac{\partial \zeta}{\partial t} = 0 \tag{25}$$

subject to the equality of sea level and cross-shelf flux at the shelf break (x = 0). The results are

$$U = \frac{-i\omega\beta e^{lx} e^{i\omega t}}{f^2 - \omega^2} \tag{26}$$

$$V = \frac{f\beta e^{lx} e^{i\omega t}}{f^2 - \omega^2} \tag{27}$$

$$\zeta = \frac{\beta e^{i\omega t} e^{lx}}{c^2 l} \tag{28}$$

where

$$\beta = \frac{\alpha(f^2 - \omega^2)}{\omega}. \tag{29}$$

For the two-layer coastal ocean (Fig. 2d), the solution is once again sought in terms of the barotropic and baroclinic components. Because the forcing of the ocean in this model is through the boundary condition primarily via the flux U_s (x = 0), the barotropic and baroclinic solutions are multiplied by the respective coefficients A and B.

From Eqs. (26)–(29) the barotropic response (subscript 1) is

$$\zeta_1 + \zeta_1' = A\beta e^{lx} e^{i\omega t} \tag{30}$$

$$U_1 + U_1' = \frac{-Ai\omega\beta e^{lx} e^{i\omega t}}{f^2 - \omega^2} \tag{31}$$

$$V_1 + V_1' = Af\beta \frac{e^{lx} e^{i\omega t}}{f^2 - \omega^2} \tag{32}$$

where Eq. (12) still applies.

The baroclinic response (subscript 2) is the solution of the equations

$$\frac{\partial U_2}{\partial t} - fV_2 = -c_0^2 \frac{\partial \zeta_2}{\partial x} \tag{33}$$

$$\frac{\partial V_2}{\partial t} + fU_2 = 0 \tag{34}$$

$$\frac{\partial U_2}{\partial x} = -\frac{h'}{\epsilon(h + h')} \frac{\partial \zeta_2}{\partial t} \tag{35}$$

subject to

$$U_2 = BU_{s\,(x=0)} = iB\alpha e^{i\omega t}, \quad \text{at} \quad x = 0 \tag{36}$$

where $c_0^2 = gh$.

The results are

$$U_2 = -U_2' = -\frac{B\beta i\omega e^{i\omega t}}{f^2 - \omega^2} e^{l_2 x} e^{i\omega t} \tag{37}$$

$$V_2 = -V_2' = \frac{B\beta e^{l_2 x} e^{i\omega t}}{f^2 - \omega^2} \tag{38}$$

$$\zeta_2 = -\epsilon \frac{h'}{h + h'} \zeta_2' = B\beta \frac{e^{l_2 x} e^{i\omega t}}{c_0^2 l_2} \tag{39}$$

where

$$l_2 = -(f^2 - \omega^2)^{1/2} / [g\epsilon h(h + h')/h']^{1/2}. \tag{40}$$

The two boundary conditions from which one determines the values of A and B are that there is no flow in and out of the vertical slope facing the bottom oceanic layer, and that the cross-shelf fluxes over the shelf and in the upper oceanic layer are equal at the shelf break, e.g.

$$U_1' + U_2' = 0 \quad \text{at} \quad x = 0 \tag{41}$$

$$U_s = U_1 + U_2 \quad \text{at} \quad x = 0. \tag{42}$$

The results are

$$B = \frac{A}{1+(h/h')} = \frac{1+(h'/h)}{2+(h/h')+(h'/h)}. \tag{43}$$

For the case of the Great Barrier Reef, $h \approx 100$ m, $h' \approx 1000$ m, $h/h' \ll 1$, and $A \approx B \approx 1$.

Hence, at the lowest order in (h/h'), the combined solution is

$$U \approx -i\alpha e^{i\omega t} e^{l_2 x} \tag{44}$$

$$V \approx \frac{f\alpha e^{i\omega t}}{\omega}(e^{lx} + e^{l_2 x}) \tag{45}$$

$$V' \approx \frac{f\alpha e^{i\omega t}}{\omega}(e^{lx} - e^{l_2 x}) \tag{46}$$

$$U' \approx -i\alpha e^{i\omega t}(e^{lx} - e^{l_2 x}) \tag{47}$$

$$\zeta' \approx \frac{\beta(h+h')}{\epsilon h' c_0^2 l_2} e^{l_2 x} e^{i\omega t} + \frac{\beta e^{lx} e^{i\omega t}}{\{1+[h'/(h+h')]\}c^2 l}. \tag{48}$$

The scaling yields $\zeta \approx 0$ at first order in h/h', justifying a posteriori the assumptions behind the model. These equations reproduce a number of observations of classical upwellings, namely the following. From Eq. (44), the cross-shelf current in the top layer $(=U/h)$ is measurable and out-of-phase with the wind, provided x is a real number. From Eq. (45), since $f/\omega \gg 1$, the longshore current in the top layer $(=V/h)$ is much larger than the cross-shelf one and in phase with the wind, provided α is a real number. From Eqs. (46) and (47), since $h' \gg h$, the wind-driven currents in the bottom layer $(U'/h', V'/h')$ are much smaller (with the ratio h/h') than those in the top layer, suggesting that the former may not be readily measurable. From Eq. (48), the thermocline is raised and lowered in phase with the wind, provided α is a real number.

Also, from Eqs. (44) and (45), it follows that the ratio U/V is time-independent, implying that the wind-driven currents in the upper layer do not rotate.

The model, because it yields such simple closed-form solutions, adds a number of findings, e.g., the barotropic and baroclinic components contribute equally to the depth-integrated currents. However, the baroclinic component dominates the thermocline displacement. One interesting finding is that bottom friction on the shelf may have a prominent influence not only on the currents on the continental shelf itself (Schwing et al., 1985) but also on the adjoining upper continental slope.

3. Some observations

In this section, observations of low-frequency oscillations of currents and temperature on the Great Barrier Reef slope are compared with the observations. The data is very sparse, limited indeed to only two current meters, and is obviously insufficient to test a theory of coastal dynamics. The shelf of the Great Barrier Reef of Australia extends for about 2000 km in a longshore direction. The shelf in the area is typically about 100 km wide and about 50 m deep (Fig. 1). In the outer 10 km of the shelf, the sea floor steepens much more rapidly to the 100 m isobath where a very steep continental slope begins (Fig. 1). The depth in the adjacent ocean basin (the Coral Sea) is about 1200 m.

No front or marked cross-shelf temperature gradient separates the surface waters of the Coral Sea from the outer shelf waters. Instead, the waters are vertically well-mixed especially in winter down to about 100 m. Hence, as is sketched in Fig. 1, the bottom of the mixed layer, which is loosely called the thermocline hereafter, is generally slightly below the shelf break elevation, i.e., the thermocline is found just offshore from the shelf itself virtually at the shelf break. Previous current meter studies by various investigators have focused on the shelf itself with no study of the dynamic coupling between the well-mixed shelf and the stratified ocean (see the reviews by Andrews, Church, Middleton, Pickard, Tomczak and Wolanski, in Baker et al., 1983).

A mooring was maintained for one year at site N, on the 180 m isobath, comprising Aanderaa current meters at 70 and 150 m below the surface, i.e., above and below the bottom of the mixed layer (Fig. 1). Sea level data were also obtained from an Aanderaa water level recorder deployed in 10 m depth at nearby Myrmidon Reef, and wind data at Rib Reef on the midshelf (Fig. 1).

Clearly, greater horizontal and vertical resolution is needed to validate the model. However, even with only one mooring, it appears that the model might be somewhat justified and at least gives an hypothesis of likely dynamics at the shelf break of the Great Barrier Reef.

All variables refer to their low-frequency components obtained by filtering the decimated hourly data using Godin's $A_{24}^2 A_{25}$ filter (period ≥ 2.8 days). The oceanographic convention is used throughout including the wind, i.e., the direction of the wind vector is taken to be the one towards which the air is blowing. Coherence levels were estimated following Thompson (1979).

The autospectra (Fig. 3) of both the longshore and cross-shelf wind components show increasing variance for increasing period. Figure 3 also illustrates the dominance, by nearly an order of magnitude, of the longshore component over the cross-shelf one.

The record of the 70 m depth current meter at site N has a gap, in summer, but two time series each four months long are still available in winter.

In Fig. 4 are shown time series plots of the wind, sea level, currents and temperature. Figure 4 (line b) suggests the presence of a mean poleward current ($\approx$20 cm s^{-1} in 1983, but not in 1984; the East Australian Current) at 70 m modulated by strong fluctuations up to 50 cm s^{-1} in amplitude with periods between 10 and 20 days. The longshore current fluctuations at 150 m (Fig. 4, line d), are much smaller than those at 70 m.

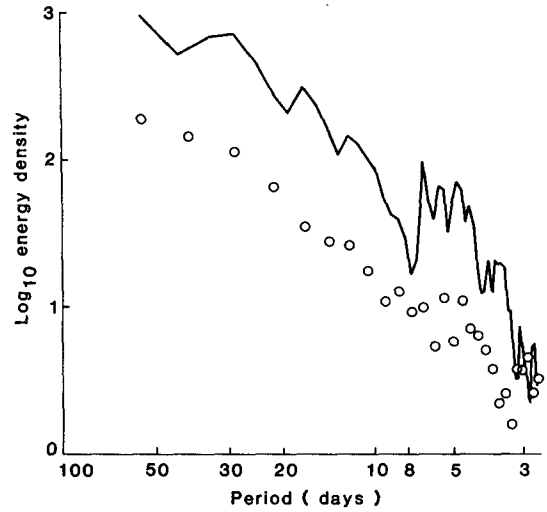

FIG. 3. Autospectra of longshore (——) and cross-shelf (O) wind components. The energy density has units $m^2 s^{-2} (cpd)^{-1}$. The 95% confidence level bars span about half a decade.

The East Australian Current is not apparent at 150 m, as indeed a mean equatorward current of about a few cm s^{-1} prevailed (Fig. 4, line d). This latter finding disagrees somewhat with that of Church and Boland (1983) who found, on the basis of geostrophic calculations, that the East Australian Current extends down to 200–250 m. The reason for this discrepancy is unknown.

A visual examination of Fig. 4 (lines a and b) suggests that the longshore current fluctuations at 70 m are coherent with the longshore wind fluctuations. Figure 4 also suggests that the cross-shelf current fluctuations at 70 m (line c) are much smaller than the longshore ones (line b), and appear to be anticorrelated with the longshore wind fluctuations (line a).

The sea level fluctuations (Fig. 4, line e) are ≤4 cm peak to trough, superimposed on a larger seasonal fluctuation. These sea level fluctuations are much smaller than those (up to 35 cm peak to trough) observed on the inner shelf (Wolanski and Bennett, 1983; Wolanski and Pickard, 1985).

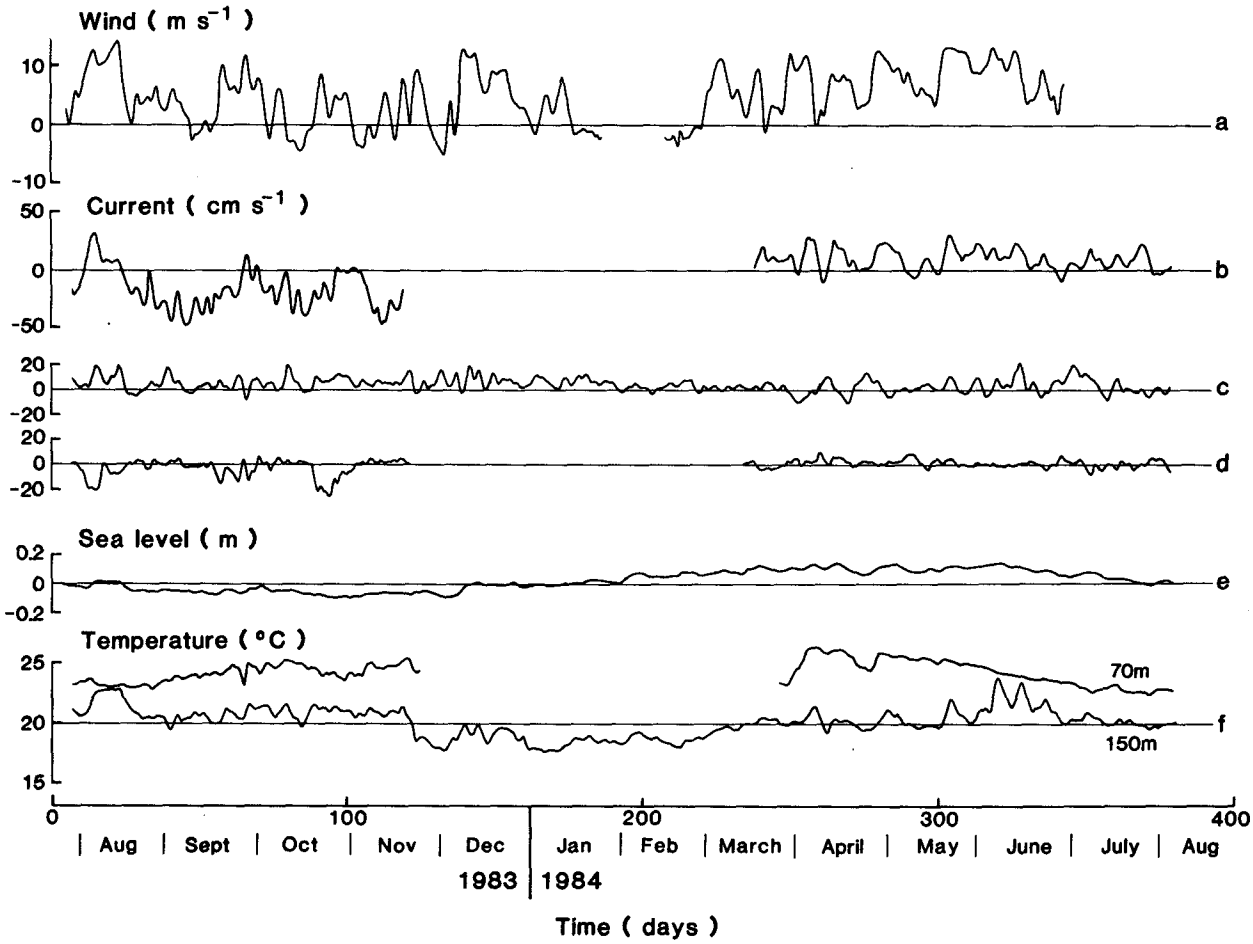

FIG. 4. Time series plot of the longshore wind component (line a, positive for northward wind), longshore current at 70 m (line b, positive for northward current) and 150 m (line c), cross-shelf current at 70 m (line d, positive for eastward current), sea level (line e), and temperature (line f) at 70 and 150 m at site N.

The plot of the temperature fluctuations (Fig. 4, line f) shows a number of events, some common to both the 70 and 150 m current meters, some showing significant fluctuations only in the bottom layer and not in the top layer. The latter are suggestive of baroclinic waves presumably trapped on the continental slope, and periodically raising and lowering the thermocline.

To determine the various relationships between wind, current and temperature, suggested in Fig. 4, the coherence and phase relationships between these variables were computed. Figure 5 (line a) shows the coherence between longshore current at 70 m and the longshore wind, implying that the wind modulates the current with a lag that is small at low frequencies but takes increasing values with increasing frequencies. The coherence between cross-shelf currents at 70 m and the longshore wind (line b in Fig. 5) is also significant, but this time nearly a 90° lag prevails. There exists a much smaller coherence (not shown) between cross-shelf current at 70 m and the cross-shelf wind, suggesting that the longshore wind is the controlling wind component. The temperature at 70 m is found to be incoherent with either the longshore or cross-shelf wind components, but this finding is not surprising since the upper layer is particularly well-mixed during trade winds. However, the temperature at 150 m is significantly coherent with the longshore wind component, for small values of the lag (Fig. 6) so that these two

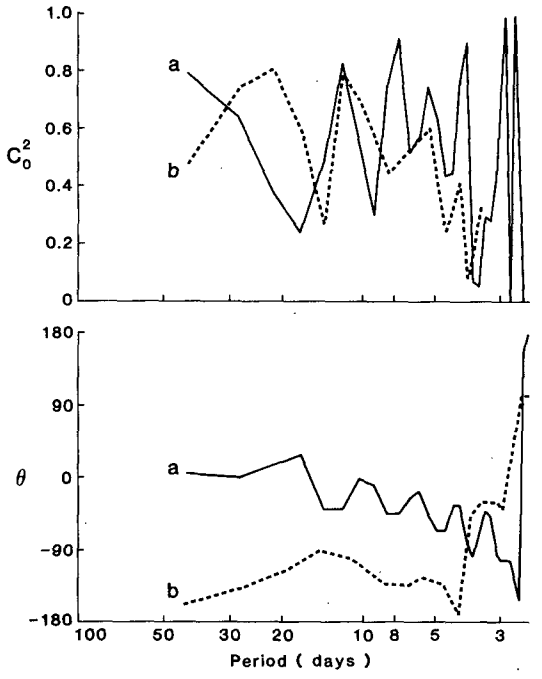

FIG. 5. Variation with period of the coherence squared (C_0^2) and phase (θ) between the longshore current at 70 m depth and the longshore wind (a), and between cross-shelf current at 70 m depth and the longshore wind (b). The 95% coherence level $\approx$ 0.4. A negative phase indicates that the current lags the wind.

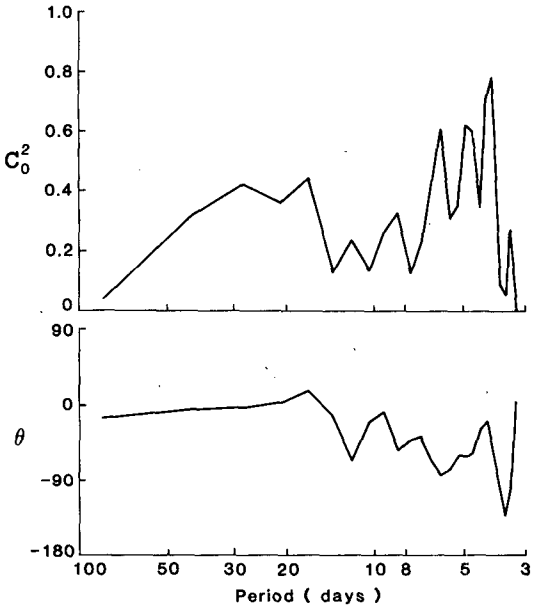

FIG. 6. Variation with period of the coherence squared (C_0^2) and phase (θ) between the temperature at 150 m and the longshore wind component. The 95% coherence level $\approx$ 0.3. A negative phase indicates that the temperature lags the wind.

parameters are nearly in phase at low frequencies. The phase relationships generally agree qualitatively with the model. For instance, the longshore current in the top layer (line a in Fig. 5) lags the wind. The lag is quite small at very low frequencies but increases at higher frequencies, a result of Eqs. 22 and 45. This general trend also holds for the temperature (Fig. 6), as predicted by equations 22 and 48. In fact, a 45° lag should occur when $\omega \approx r$. From the field data, this lag occurs at period $T = 2\pi/\omega \approx 5$ days, leading to a new estimate of the value of $r = 1.5 \times 10^{-5}$ s^{-1}, a value which falls in range of the previously estimated values. This new estimate of r is somewhat speculative in view of the neglect of the sea floor slope of the shelf. This slope is of order 6×10^{-4}, which is greater than the critical slope $f(rh_s/g\omega)^{1/2} \approx 3 \times 10^{-4}$, for $T = 20$ days, above which other forces than friction are important (Schwing et al., 1985). However, on the shelf, the friction parameter may not necessarily decrease with increasing depth because of the corresponding increasing reef density. The phase relationship between temperature and cross-shelf currents should show theoretically a 90° phase at very low frequencies, but, while a large phase is observed, the predictions are not particularly well reproduced. Note also that the wind-driven currents at 70 m do not rotate as the clockwise and anticlockwise rotating components of the spectra (Fig. 7) are practically equal, i.e. the currents are highly rectilinear. This observation is also qualitatively in agreement with the model.

If we idealize the situation by assuming a two-layer ocean (see Fig. 2d) these observations suggest that, un-

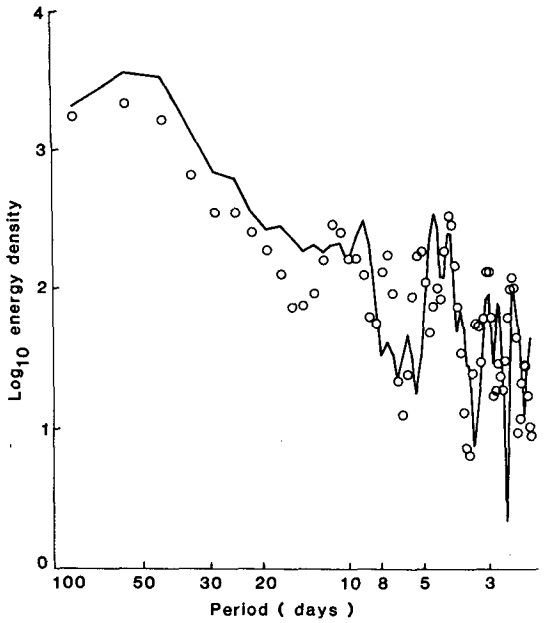

FIG. 7. Rotational spectrum (clockwise rotating = line; anticlockwise rotating = circles) of the currents at 70 m depth at site N. The energy density has units $cm^2\ s^{-2}\ (cpd)^{-1}$.

der the action of reversing longshore wind, reversing longshore currents result with little lag in the top layer, but these currents are too small to be measured in the bottom layer. At the shelf break, sea level fluctuations are small. During these current fluctuations, the temperature in the top layer does not change much (since it is a well-mixed layer), but the thermocline is alternately raised and lowered. A comparison of the temperature time series with the vertical profiles of temperature suggests a maximum vertical amplitude of the thermocline of order 50 m. If these baroclinic waves spill into the shelf, the model suggests they would be quite extensive in the longshore direction, a finding that is consistent with the unexplained observations of Andrews and Furnas (1986) that the intrusion can be coherent over at least 200 km in the longshore direction.

This model theoretically should be applicable to other regions that geometrically match the Great Barrier Reef, i.e. a wide, shallow homogeneous shelf, no buoyancy differences between surface waters on the shelf and the slope, and a thermocline intersecting into a steep slope. The model is thus not applicable to the South Atlantic Bight where the variability in the outer shelf is dominated by baroclinic events of Gulf Stream origin (Lee et al., 1984). The model however may find applications to the North West shelf of Australia. There, though the upper slope data is also sparse, Holloway and Nye (1985) and Holloway et al. (1985) found that when the wind fluctuations reverse the direction of the current on the outer shelf, from southward to northward, a subsurface intrusion of deep water (i.e. an upwelling) is experienced in the weather bands, even in winter when the thermocline intersects the steep continental slope.

4. Discussion

A simple analytical model, sketched in Fig. 2d, is proposed that explains qualitatively well the various coherence and phase relationships that one could expect in classical upwelling situations such as the one at the shelf break of the Great Barrier Reef where, however, the data is too sparse for a detailed verification of the model. On this basis, the upwelling events may be controlled by the coupling between the stratified slope waters and the well-mixed shelf waters with periodically reversing wind-driven currents.

The model is extremely simple but may be reasonable. Though the model is only a logical extension of the classical upwelling models of Gill and Clarke (1974), Kajiura (1974), Csanady (1982) and Clarke and Brink (1985), it has the advantage that it yields a simple explicit closed-form solution. This solution shows the separate but interacting roles of the barotropic and baroclinic components of the shelf break dynamics. The model suggests that bottom friction on the continental shelf may play a dominant role in upwelling on the continental slope.

A number of other effects, the importance of which is unknown, may also be important in the upwelling dynamics on the Great Barrier Reef, such as forcing from events in the Coral Sea, leaky waves, the finite sea bed slope offshore from the shelf break, the stratification of the water below the thermocline (so that many modes of oscillations can be excited), and the longshore structures in the topography of the slope. Clearly, to resolve the dynamics at the Great Barrier Reef shelf break, extensive current meter records are needed.

Acknowledgments. It is a pleasure to acknowledge the assistance of Dr. R. Strickler, Mr. R. McAllister, Ms. M. Thyssen and Mr. J. Futcher. Dr. P. Holloway and an anonymous reviewer criticized and improved the manuscript.

REFERENCES

Allen, J. S., 1980: Models of wind-driven currents on the continental shelf. *Annual Reviews in Fluid Mechanics,* Vol. 12, Annual Reviews, 389–433.

Andrews, J. C., and M. J. Furnas, 1986: Subsurface intrusions of Coral Sea water into the central Great Barrier Reef. I: Structures and shelf-scale dynamics. *Contin. Shelf Res.,* **5** (In press).

Baker, J. T., R. M. Carter, P. W. Sammarco and K. P. Stark, (Eds.), 1983: *Proc. of the Inaugural Great Barrier Reef Conf.,* Townsville, James Cook University Press, 545 pp.

Church, J. A., and F. M. Boland, 1983: A permanent undercurrent adjacent to the Great Barrier Reef. *J. Phys. Oceanogr.,* **13,** 1747–1749.

——, J. C. Andrews and F. M. Boland, 1985: Tidal currents in the central Great Barrier Reef. *Contin. Shelf Res.,* **4,** 515–531.

Clarke, A. J., and K. H. Brink, 1985: The response of stratified fric-

tional shelf and slope waters to fluctuating large-scale low-frequency wind forcing. *J. Phys. Oceanogr.*, **15,** 439–453.

Csanady, G. T., 1982: *Circulation in the Coastal Ocean.* Reidel, 279 pp.

Gill, A. E., and A. J. Clarke, 1974: Wind-induced upwelling, coastal currents and sea-level changes. *Deep-Sea Res.*, **21,** 325–346.

Holloway, P. E., and H. C. Nye, 1985: Leeuwin current and wind distributions on the southern part of the Australian North West Shelf between January 1982 and July 1983. *Aust. J. Mar. Freshwater Res.*, **36,** 123–137.

——, S. E. Humphries, M. Atkinson and J. Imberger, 1985: Mechanisms for nutrient supply to the Australian North West Shelf. *Aust. J. Mar. Freshwater Res.*, **36,** 753–764.

Kajiura, K., 1974: Effect of stratification on long period trapped waves on the shelf. *J. Oceanogr. Soc. Japan,* **30,** 271–281.

Lee, T. N., W. J. Ho, V. Kourafalou and J. D. Wang, 1984: Circulation on the continental shelf of the southeastern United States. Part I: Subtidal response to wind and Gulf Stream forcing during winter. *J. Phys. Oceanogr.*, **14,** 1001–1012.

Lewis, J. K., and R. O. Reid, 1985: Local wind forcing of a coastal sea at subinertial frequencies. *J. Geophys. Res.*, **90,** 935–944.

Middleton, J. H., and R. E. Thomson, 1985: Steady wind-driven coastal circulation on a β-plane. *J. Phys. Oceanogr.*, **15,** 1809–1817.

Mysak, L. A., 1980: Topographically trapped waves. *Annual Review in Fluid Mechanics,* Vol. 12, Annual Reviews, 45–76.

Schwing, F. B., L.-Y. Oey and J. O. Blanton, 1985: Frictional response of continental shelf water to local wind forcing. *J. Phys. Oceanogr.*, **15,** 1733–1746.

Thompson, R. O. R. Y., 1979: Coherence signal levels. *J. Atmos. Sci.*, **36,** 2020–2021.

Wolanski, E., 1982: Low level trade winds over the western Coral Sea. *J. Appl. Meteor.*, **21,** 881–882.

——, and A. F. Bennett, 1983: Continental shelf waves and their influence on the circulation around the Great Barrier Reef. *Aust. J. Mar. Freshwater Res.*, **34,** 23–47.

——, and R. E. Thomson, 1984: Wind-driven circulation on the northern Great Barrier Reef continental shelf in summer. *Estuarine, Coastal and Shelf Sci.*, **18,** 271–289.

——, and G. L. Pickard, 1985: Long-term observations of currents on the central Great Barrier Reef continental shelf. *Coral Reefs,* **4,** 47–57.

——, J. Imberger and M. L. Heron, 1984: Island wakes in shallow coastal waters. *J. Geophys. Res.*, **89,** 10553–10569.